



Performance analysis of adaptive M-QAM over a flat-fading Nakagami- m channel

Authors:

Tahmid Quazi¹
HongJun Xu¹

Affiliation:

¹School of Electrical, Electronic and Computer Engineering, University of KwaZulu-Natal, Durban, South Africa

Correspondence to:

Tahmid Quazi

email:

quazit@ukzn.ac.za

Postal address:

School of Electrical, Electronic and Computer Engineering, University of KwaZulu-Natal, King George V Avenue, Durban 4001, South Africa

Dates:

Received: 22 Jan. 2010

Accepted: 18 Oct. 2010

Published: 28 Jan. 2011

How to cite this article:

Quazi T, Xu H. Performance analysis of adaptive M-QAM over a flat-fading Nakagami- m channel. *S Afr J Sci*. 2011;107(1/2), Art. #122, 7 pages. DOI: 10.4102/sajs.v107i1/2.122

© 2011. The Authors.
Licensee: OpenJournals Publishing. This work is licensed under the Creative Commons Attribution License.

Channel adaptive M-ary quadrature amplitude modulation (M-QAM) schemes have been developed to provide higher average link spectral efficiency by taking advantage of the time-varying nature of wireless fading channels. Much of the earlier work on such schemes uses the assumption that thresholds designed for additive white Gaussian noise (AWGN) channels can be directly applied to slowly varying block-fading channels. The thresholds are calculated with a commonly used approximation bit error rate (BER) expression in these schemes. The first aim of this paper was to investigate the accuracy of using this common BER expression in a fading channel. This was done by comparing the result of the average BER expression derived using the approximate expression with results of simulations over a Nakagami- m block-fading channel. The second aim was to show that the inaccuracy in the threshold values determined using the closed form approximation expression would lead to inappropriate operation of the adaptive M-QAM scheme in a fading channel. This was done by comparing expected theoretical values with the simulation results. Two alternative approximate BER expressions for M-QAM in AWGN were then presented and used to determine the average M-QAM of BER over a Nakagami- m fading channel. The comparison between the average BER expressions and the simulation showed a much closer match. More accurate thresholds for the adaptive M-QAM system were then determined using one of the two average BER expressions and the accuracy of these threshold points was then verified using simulation results.

Introduction

In order to achieve quality of service (QoS) targets such as bit error rate (BER) and throughput in a point-to-point wireless fading channel, it is critical to maximise the spectral efficiency of the transmissions. One of the ways to achieve this is to use a channel adaptive modulation scheme. In particular, adaptive M-ary quadrature amplitude modulation (M-QAM) schemes have been used because they allow high data rate transmissions without increasing the bandwidth of wireless communications systems.

Discrete-rate M-QAM has been applied to various channel adaptive transmission schemes. The objective of all of these schemes is to enhance the spectral efficiency of the transmissions by using M-QAM to adapt the transmission rate to a time-varying fading channel. Previous research^{1,2,3} has demonstrated the improvement in spectral efficiency of the adaptive system while achieving a specified QoS BER target in the operable signal-to-noise ratio (SNR) range. Further research^{4,5,6,7} improved the performance of the adaptive system by combining coding with rate adaptive M-QAM. Some schemes^{8,9,10} used an adaptive M-QAM and coding system in the physical layer module of the proposed cross-layer design mechanisms. The adaptive physical layer was combined with the data link layer by Liu and colleagues^{8,9} while in another study¹⁰ it was combined with the application layer. Previous studies^{11,12,13,14} combined M-QAM adaptive modulation to the diversity combining technique to propose schemes where the modulation mode and the diversity combiner structure are adaptively determined based on the channel fade condition and the error-rate requirement. Nechiporenko et al.¹⁵ analysed the performance of an amplified and forward co-operative system with constant-power, rate-adaptive M-QAM transmission.

In the system design and performance analysis in most of the previous studies,^{1,3,4,10,11,12,14,15} the derivation of the system BER was done using a common approximate expression for BER of M-QAM in additive white Gaussian noise (AWGN).¹ This expression is used to derive the average BER expression for the performance analysis of these systems in a fading channel. Additionally, this simple closed form BER expression has been used to determine the SNR boundaries of the adaptive system. An assumption in all the studies cited above is that the threshold values, determined using an AWGN BER expression, can be used for the adaptive system in a fading



channel because slowly fading block-fading channels can be modelled as AWGN channels. Most of these studies present the BER performance of the system over a Nakagami- m fading channel using only theoretical analysis and only Goldsmith and Chua³ presented system simulations. Although the Goldsmith and Chua³ study is an exception, the performance curves show that there is a significant gap between the analytical expression and the simulation result. Goldsmith and Chua³ explain that the gap exists as a result of choosing overly conservative design values for the threshold points. Nechiporenko et al.¹⁵ also confirmed this statement and mentioned that the threshold can be further optimised. The motivation for this paper is to investigate the accuracy of the common BER expression in a fading channel and the accuracy of the assumption that threshold values designed for AWGN channels can be used in Nakagami- m fading channels.

System model

The transmission rate on the point-to-point wireless fading channel is adaptively adjusted by utilising an adaptive modulation scheme as shown in Figure 1.

In the modulation mode controller of Figure 1, Gray coded discrete (square and rectangular) M-ary QAM modes with $M := 2^n (n = 2, 3, \dots, N)$ are used for the channel adaptive scheme. The transmissions are assumed to be over a slowly varying flat-fading channel with the fading assumed to follow a Nakagami- m distribution. This corresponds to a block-fading model, where the rate adjustment occurs on a frame-by-frame basis. The signal at the receiver is perturbed by AWGN which is modelled as a zero-mean complex Gaussian random variable with variance $N_0/2$ per dimension, where N_0 is the single-sided power spectrum density of the noise. It is assumed that perfect channel estimation is possible at the receiver and that the feedback channel is instantaneous and error free.

At the receiver, the received signal is given by $r = at + gn$ where a is the Nakagami- m fading co-efficient with the probability density function (pdf) given by [Eqn 1], t is the transmitted signal and gn is the AWGN.

$$p_\alpha(\alpha) = \frac{2}{\Gamma(m)} \left(\frac{m}{\Omega}\right)^m \alpha^{2m-1} \exp\left(-\frac{m\alpha^2}{\Omega}\right) \quad [\text{Eqn 1}]$$

where m is the Nakagami fading parameter and $\Gamma(m)$ is the Gamma function defined by $\Gamma(m) = \int_0^\infty y^{m-1} \exp(-y) dy$ and $\Omega = E[|\alpha|^2]$, E being the expectation. Define the received instantaneous SNR as

$$\gamma = \frac{|\alpha|^2 E_s}{N_0} \quad [\text{Eqn 1}]$$

(E_s is the symbol energy). For a Nakagami- m fading channel, then the pdf of γ is given by¹:

$$p_\gamma(\gamma) = \left(\frac{m}{\bar{\gamma}}\right)^m \frac{\gamma^{m-1} \exp\left(-\frac{m\gamma}{\bar{\gamma}}\right)}{\Gamma(m)}, \gamma \geq 0 \quad [\text{Eqn 2}]$$

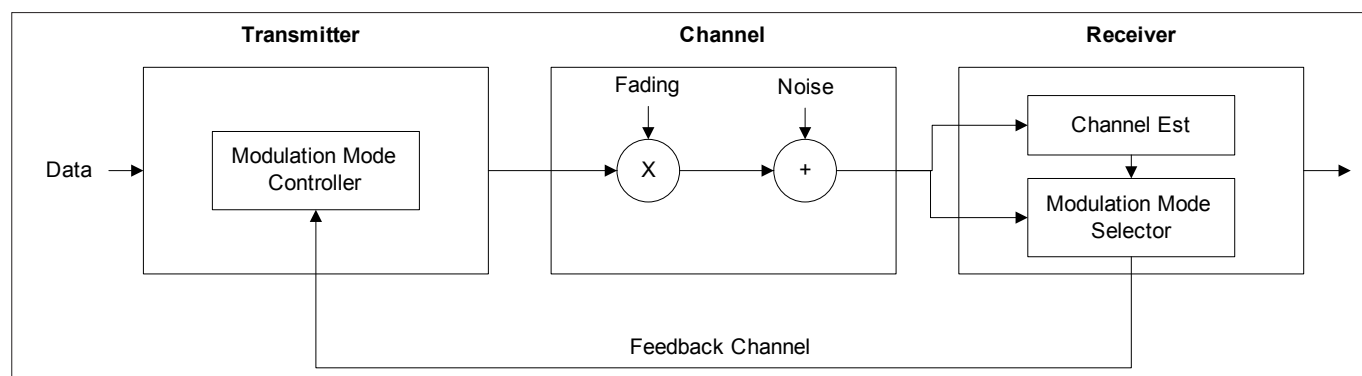
where

$$\bar{\gamma} = E[\gamma] = \Omega \frac{E_s}{N_0} \quad [\text{Eqn 3}]$$

The received SNR range is split into $(N + 1)$ fading regions (bins), with region n having a corresponding mode M_n . The set $\{\gamma_n\}_{n=2}^N$ contains the lower thresholds for the N fading regions, calculated such that the target BER (referred to as BER_0) is achieved for each M_n -QAM modulation scheme. γ_1 is set to 0 dB and γ_{N+1} to ∞ . Thus when the received instantaneous SNR, γ , falls within region n ($\gamma_n \leq \gamma < \gamma_{n+1}$), the associated fading index n is sent back to the transmitter through a dedicated feedback channel. To avoid deep fades, no data is sent when $\gamma_1 \leq \gamma < \gamma_2$ (outage). The design of the threshold set $\{\gamma_n\}_{n=2}^N$ will be discussed in subsequent sections.

Limitations of previous designs

Goldsmith and colleagues^{1,3,4} investigated the application of adaptive schemes for improving the spectral efficiency of transmissions over fading channels. The schemes presented by them used the premise that adaptive schemes originally designed for AWGN channels can be used over a fading channel. In this section we investigate the merits of this assertion. The adaptive schemes in other studies^{1,3,4,10,11,12,14,15} used the approximation expression shown in [Eqn 4] for the BER of coherent M-QAM with two-dimensional Gray coding over the AWGN channel.¹



Source: Goldsmith and Chua³

FIGURE 1: Adaptive M-ary quadrature amplitude modulation system model.



$$P_b(\gamma) \approx 0.2 \exp\left(\frac{-3\gamma}{2(M-1)}\right) \tag{Eqn 4}$$

We have used this expression in our previous work,¹⁰ where a channel adaptive physical layer and application layer cross-layer design were applied. The performance analysis was done for multimedia data transmission over an AWGN channel.¹⁰ However, when an attempt was made to extend the analysis to study the performance of the rate adaptive scheme (at the physical layer first) over a fading channel, a noticeable mismatch was found between the analysis and simulation curves. There was a shift of up to 4 dB when the SNR was higher than 20 dB. Upon further study of the performance graphs in Alouini and Goldsmith's¹ and Goldsmith and Chua's³ studies, a similar trend was found. In Alouini and Goldsmith's study,¹ the shift was between an 'exact average BER' computation and that computed using [Eqn 4]. In Goldsmith and Chua's study,³ the gap was found between the simulation and the analysis. The only explanation the authors offered is that their analytical calculations are pessimistic and that there is room for further efficiency while still maintaining the target BER of 1×10^{-3} . It will now be shown that the approximate expression in [Eqn 4], although useful for an AWGN channel, is significantly inaccurate for Nakagami- m fading channels.

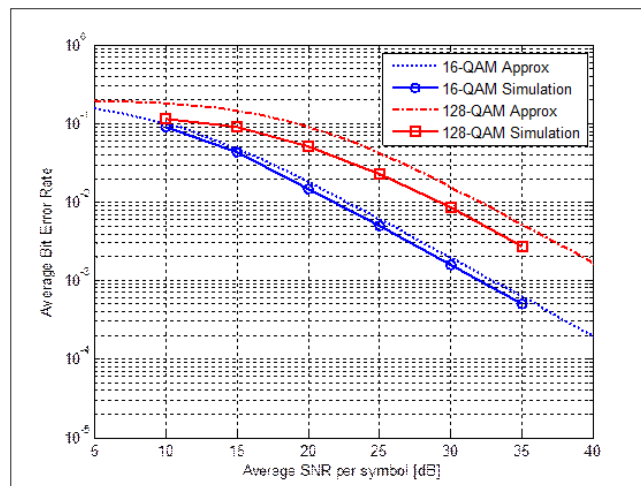
If t is assumed to be the transmitted signal, the received signal in an AWGN channel is given by $r = t + gn$, where gn represents the noise factor. The BER for M-QAM is then given by [Eqn 4]. The average BER in a slow and flat Nakagami- m fading channel may be derived by averaging the error rates for the AWGN channel over the pdf of the SNR in Nakagami- m fading:

$$\begin{aligned} P_b(\bar{\gamma}) &= \int_{-\infty}^{\infty} P_b(\gamma) \times p_{\gamma}(\gamma) d\gamma \\ &= \int_0^{\infty} 0.2 \exp\left(\frac{-3\bar{\gamma}}{2(M-1)}\right) \times \left(\frac{m}{\bar{\gamma}}\right)^m \frac{\bar{\gamma}^{m-1} \exp(-\frac{m\bar{\gamma}}{\gamma})}{\Gamma(m)} d\bar{\gamma} \\ &= \frac{0.2}{\Gamma(m)} \left(\frac{m}{\bar{\gamma}}\right)^m \int_0^{\infty} \gamma^{m-1} \exp(-\gamma\beta) d\gamma \end{aligned} \tag{Eqn 5}$$

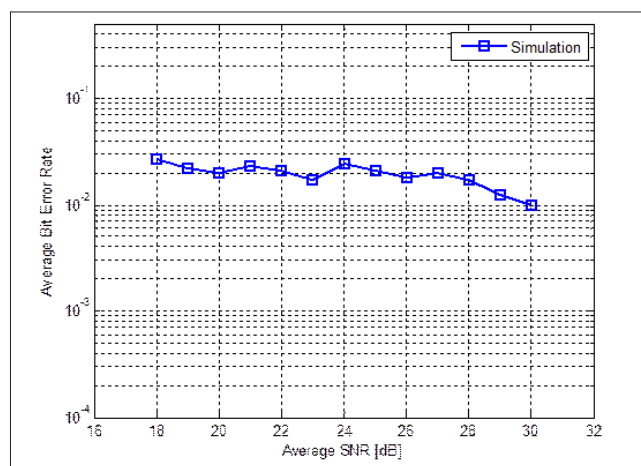
where $\beta = \frac{3\bar{\gamma} + 2m(M-1)}{2(M-1)\bar{\gamma}}$, and $\bar{\gamma}$ is the average SNR per symbol defined in [Eqn 3]. After completing the integration (refer to Appendix I) and some simplification, the following expression for the average BER can be derived:

$$P_b(\bar{\gamma}) = 0.2 \left(\frac{m}{\bar{\gamma}\beta}\right)^m \tag{Eqn 6}$$

M-QAM, with $M = 16, 32, 64$ and 128 were simulated over an $m = 1$ Nakagami- m fading channel, where Nakagami- m fading was simulated using the technique presented by Abreu¹⁶. The results of the simulations were compared to the theoretical results obtained from using the approximate average BER expression in [Eqn 6]. The first point to note from the comparison is the gap between the simulation and theory graphs for all four modulation schemes. For purposes of clarity only the graphs for $M = 16$ and $M = 128$ are shown in Figure 2. As seen in the graphs, there is a large difference (a gap of up to 4 dB) between the average BER computation



SNR, signal-to-noise ratio.
FIGURE 2: Average bit error rate of a M-ary quadrature amplitude modulation scheme over a $m = 1$ Nakagami- m fading channel using the approximation bit error rate expression in [Eqn 6].



SNR, signal-to-noise ratio.
FIGURE 3: Average bit error rate of an adaptive M-ary quadrature amplitude modulation scheme over a $m = 1$ Nakagami- m fading channel with thresholds calculated using the approximation bit error rate expression in [Eqn 6].

using [Eqn 6] and the simulation for 128-QAM and there is even a shift of approximately 1 dB for 16-QAM. The gap increases as M increases. We propose that the major reason for the performance difference between the simulation in Goldsmith and Chua's study³ ('exact' in Alouini and Goldsmith's study¹) and the analysis of the rate adaptation scheme is that the inaccuracy of the expression in [Eqn 6] makes it unsuited for a Nakagami- m fading channel.

The second point that can be observed from the study of the simulation results is the inaccuracy of the thresholds derived for an adaptive M-QAM scheme using the approximate BER expression in [Eqn 4]. If M-QAM, with $M = 16, 32, 64$ and 128 is considered, the threshold points for an adaptive M-QAM system for a target BER of 1×10^{-3} using [Eqn 4] would be 17.24 dB, 20.39 dB, 23.47 dB and 26.52 dB, respectively.^{1,10} However, the simulation results for the $m = 1$ Nakagami- m fading channel in the region from 18 dB to 30 dB in Figure 3 shows that the system BER at these points would be near 2×10^{-2} , pointing to the inaccuracy of these threshold values for the fading channel.



It is clear from the analysis of the simulation results that the expression in [Eqn 4] results in inadequate accuracy for the adaptive M-QAM system in a fading channel. This is because it is not a good approximation for the exact expression for the BER of M-QAM which uses the $Q(x)$ and $Q^2(x)$ functions. The objective in the next section is to derive more accurate approximations for these functions in order to formulate an alternative BER expression that will improve the accuracy of the adaptive M-QAM system in a fading channel.

Alternative BER derivation for M-QAM

The simulation results in the above section show that using the approximate expression in [Eqn 6] will result in inaccuracies in an adaptive M-QAM modulation scheme over a Nakagami- m fading channel. Thus a more accurate expression for the BER performance is required in order to design the adaptive scheme.

The exact symbol error rate (SER) for square M-QAM (i.e. $\log_2 M$ is even) in an AWGN channel is given by¹⁷:

$$P_s^{(even)}(\gamma) = 4 \left(1 - \frac{1}{\sqrt{M}}\right) Q\left(\sqrt{\frac{3\gamma}{M-1}}\right) - 4 \left(1 - \frac{1}{\sqrt{M}}\right)^2 Q^2\left(\sqrt{\frac{3\gamma}{M-1}}\right) \quad [\text{Eqn 7}]$$

where γ is the received SNR per symbol.¹⁸ The SER for a rectangular M-QAM ($\log_2 M$ is odd) is tightly bound by¹⁷:

$$P_s^{(odd)}(\gamma) \leq 4 \left(1 - \frac{1}{\sqrt{M}}\right) Q\left(\sqrt{\frac{3\gamma}{M-1}}\right) - 4 \left(1 - \frac{1}{\sqrt{M}}\right)^2 Q^2\left(\sqrt{\frac{3\gamma}{M-1}}\right) \quad [\text{Eqn 8}]$$

As discussed in the previous section, [Eqn 4] is not an accurate approximation for the exact BER for M-QAM in an AWGN channel. In order to formulate a more accurate approximation, two methods are considered in this section for the evaluation of the $Q(x)$ and $Q^2(x)$ functions used in [Eqn 7]. The first used the following approximations for the two functions^{19,20}:

$$Q(x) \approx \frac{1}{12} \exp\left(\frac{-x^2}{2}\right) + \frac{1}{4} \exp\left(\frac{-2x^2}{3}\right) \quad [\text{Eqn 9}]$$

$$Q^2(x) \approx \frac{1}{8} \exp(-x^2) \quad [\text{Eqn 10}]$$

Applying [Eqn 9] and [Eqn 10] into [Eqn 7], the SER for M-QAM in AWGN is given by:

$$P_s(\gamma) \approx a \left\{ \exp\left(\frac{-2b\gamma}{3}\right) + \frac{\exp\left(\frac{-b\gamma}{2}\right)}{3} - \frac{a \times \exp(-b\gamma)}{2} \right\} \quad [\text{Eqn 11}]$$

$$\text{where } a = \left(1 - \frac{1}{\sqrt{M}}\right), b = \frac{3}{(M-1)} \text{ and } \gamma = \frac{E_s}{N_0}$$

This is referred to as Method 1 in the rest of the paper.

For the second method, the $Q(x)$ and $Q^2(x)$ functions are defined as¹⁸:

$$Q(x) = \frac{1}{\pi} \int_0^{\pi/2} \exp\left(\frac{-x^2}{2\sin^2\theta}\right) d\theta \quad [\text{Eqn 12}]$$

$$Q^2(x) = \frac{1}{\pi} \int_0^{\pi/4} \exp\left(\frac{-x^2}{2\sin^2\theta}\right) d\theta \quad [\text{Eqn 13}]$$

[Eqn 12] and [Eqn 13] cannot be evaluated in a closed form, however, the integration can be computed using a numerical integration. The trapezoidal rule for numerical integration is given as follows:

$$\int_a^b f(x) \approx \frac{b-a}{n} \left[\frac{f(a)+f(b)}{2} + \sum_{k=1}^{p-1} f\left(a+k\frac{b-a}{n}\right) \right] \quad [\text{Eqn 2}]$$

where p is the number of summations. After applying the trapezoidal rule to [Eqn 12], the following expression is derived²⁰:

$$Q_p(x) \approx \frac{\exp\left(\frac{-x^2}{2}\right)}{4p} + \frac{1}{4p} \sum_{i=1}^{p-1} \exp\left(\frac{-x^2}{2\sin^2\theta_i}\right) \quad [\text{Eqn 14}]$$

where $\theta_i = \frac{i\pi}{2p}$

$Q^2(x)$ can be derived using a similar process and is given by²⁰:

$$Q_p^2(x) \approx \frac{\exp(-x^2)}{8p} + \frac{1}{4p} \sum_{i=1}^{p-1} \exp\left(\frac{-x^2}{2\sin^2\theta_i}\right) \quad [\text{Eqn 15}]$$

$$\text{where } \theta_i = \frac{i\pi}{4p}$$

It was shown by Al-Shahrani²⁰ that applying a p larger than 6 results in a perfect match between the exact simulation and the numerical computation for [Eqn 7] and [Eqn 8]. Applying [Eqn 14] and [Eqn 15] into [Eqn 7] and after some simplification, the SER for M-QAM in AWGN is given by:

$$P_s(\gamma) \approx \frac{a}{p} \left\{ \frac{\exp\left(\frac{-b\gamma}{2}\right)}{2} - \frac{a \times \exp(-b\gamma)}{2} + (1-a) \sum_{i=1}^{p-1} \exp\left(\frac{-b\gamma}{S_i}\right) + \sum_{i=p}^{2p-1} \exp\left(\frac{-b\gamma}{S_i}\right) \right\} \quad [\text{Eqn 16}]$$

$$\text{where } a = \left(1 - \frac{1}{\sqrt{M}}\right); b = \frac{3}{(M-1)}; S_i = 2\sin^2\left(\frac{i\pi}{4p}\right) \text{ and } \gamma = \frac{E_s}{N_0}$$

This is referred to as Method 2 in the rest of the paper.

The average SER over a Nakagami- m fading channel is found by averaging [Eqn 11] and [Eqn 16] over the pdf of the SNR in Nakagami- m fading:

$$P_s(\bar{\gamma}) = \int_{-\infty}^{\infty} P_s(\gamma) \times p_{\gamma}(\gamma) d\gamma = \int_0^{\infty} P_s(\bar{\gamma}) \times \left(\frac{m}{\bar{\gamma}}\right)^m \frac{\gamma^{m-1} \exp\left(\frac{-m\bar{\gamma}}{\gamma}\right)}{\Gamma(m)} d\gamma \quad [\text{Eqn 17}]$$

where $\bar{\gamma}$ is defined as in [Eqn 3]. The evaluation of [Eqn 17] leads to the following closed-form expressions for the average SER, $P_s^1(\bar{\gamma})$ and $P_s^2(\bar{\gamma})$, using Method 1 and Method 2, respectively:



$$P_s^1(\bar{\gamma}) = a \left\{ \left(\frac{3m}{3m + 2b\bar{\gamma}} \right)^m + \frac{1}{3} \left(\frac{2m}{2m + b\bar{\gamma}} \right)^m - \frac{a}{2} \left(\frac{m}{m + b\bar{\gamma}} \right)^m \right\} \quad [\text{Eqn 18}]$$

$$P_s^2(\bar{\gamma}) = \frac{a}{p} \left\{ \frac{1}{2} \left(\frac{2m}{2m + b\bar{\gamma}} \right)^m - \frac{a}{2} \left(\frac{m}{m + b\bar{\gamma}} \right)^m + (1-a) \sum_{i=1}^{p-1} \left(\frac{mS_i}{mS_i + b\bar{\gamma}} \right)^m + \sum_{i=1}^{2p-1} \left(\frac{mS_i}{mS_i + b\bar{\gamma}} \right)^m \right\} \quad [\text{Eqn 19}]$$

BERs $P_b^1(\bar{\gamma})$, and $P_b^2(\bar{\gamma})$, for both Methods 1 and 2 are derived from the approximation relationship¹⁷:

$$P_b(\bar{\gamma}) \cong \frac{P_s(\bar{\gamma})}{k} \quad [\text{Eqn 3}]$$

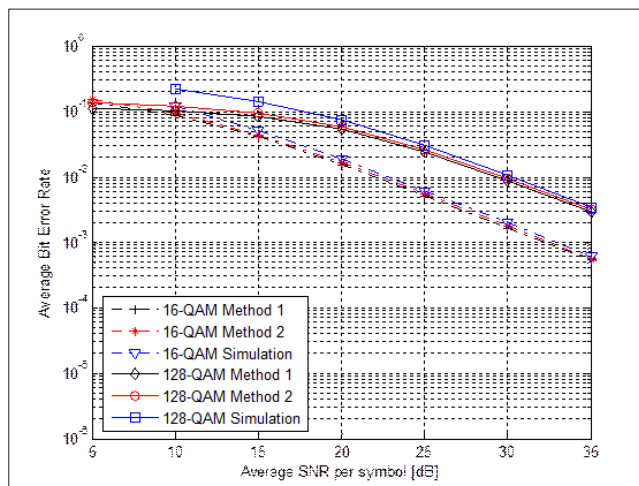
where $k = \log_2 M$ bits/symbol.

Figure 4 presents the plots of the same modulation schemes $M = 16$ and $M = 128$ used in Figure 2. However the $P_b(\bar{\gamma})$ is determined using Method 1 and Method 2. The graphs show that, when compared to the results in Figure 2, there is a much closer match between the analysis expression and the simulation result for both the methods. Thus [Eqn 20], using either method, can be more confidently used for computing the average BER of M-QAM over a Nakagami- m fading channel than using [Eqn 6].

Figure 4 shows a noticeable gap between the simulation and expected theoretical values for $M = 128$ in lower SNR regions (SNR < 17 dB). This can be attributed to the limitation of Gray coded modulation and the approximation in [Eqn 20] at low SNR values. The results in Figure 4 show that the Gray coded modulation assertion of one symbol error equating to one bit error is upheld for high SNR values. Thus, simply dividing the SER by the number of bits per symbol (k) gives an accurate BER value. However, when the SNR value is low, one symbol error could be as a result of more than one bit error, and so the division by k leads to inaccuracies. This is highlighted by the plot for $M = 128$, which has a higher number of bits per symbol than 16-QAM. This difference between the simulation and theory curves at the lower SNR region is however ignored in the design of the adaptive M-QAM system because transmission using modulation schemes with high bits per symbol, such as 64-QAM or 128-QAM, is not considered in the low SNR regions where the BER is high. It should also be noted that Method 2 produces a closer match to the simulation results when compared to Method 1.

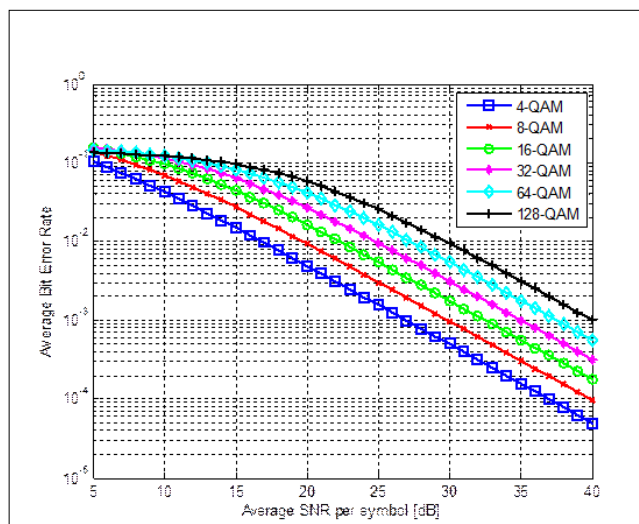
Improved adaptive M-QAM design

The next step in designing the channel adaptive M-QAM modulation scheme is to use the more accurate BER expression in [Eqn 3] to determine the SNR threshold set $\{\gamma_n\}_{n=2}^N$ for the Nakagami- m , $m = 1, 2$ and 5 fading channel for a given QoS BER target. Because of its closer match to the simulation result, Method 2 is used in the calculation of the threshold set. Using Method 2, the $P_b(\bar{\gamma})$ based on [Eqn 3]



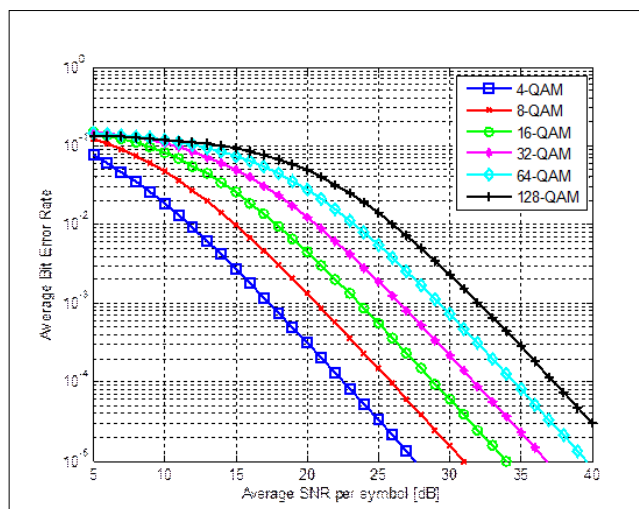
SNR, signal-to-noise ratio.

FIGURE 4: Average bit error rate of a M-ary quadrature amplitude modulation scheme over a $m = 1$ Nakagami- m fading channel derived using Method 1 and Method 2.



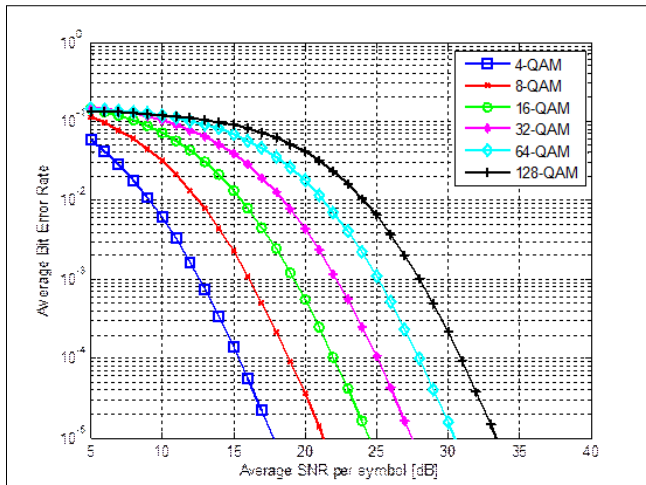
SNR, signal-to-noise ratio.

FIGURE 5: Average bit error rate for a M-ary quadrature amplitude modulation scheme over a $m = 1$ Nakagami- m fading channel.



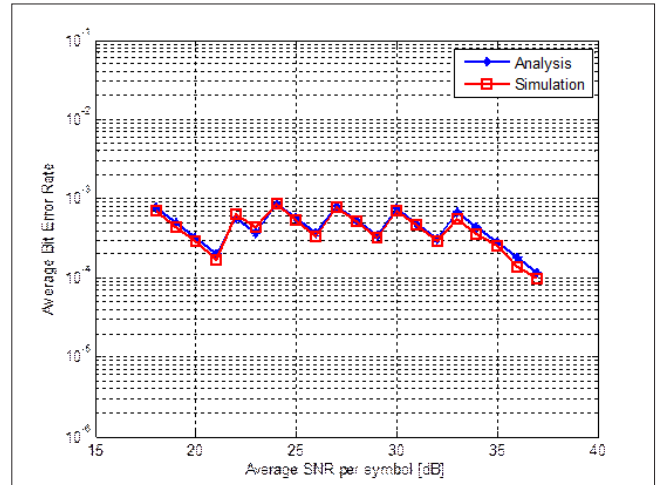
SNR, signal-to-noise ratio.

FIGURE 6: Average bit error rate for a M-ary quadrature amplitude modulation scheme over a $m = 2$ Nakagami- m fading channel.



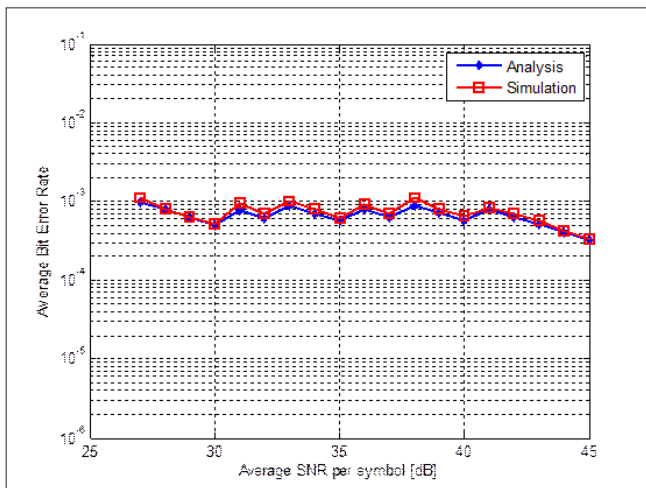
SNR, signal-to-noise ratio.

FIGURE 7: Average bit error rate for a M-ary quadrature modulation scheme over a $m = 5$ Nakagami- m fading channel.



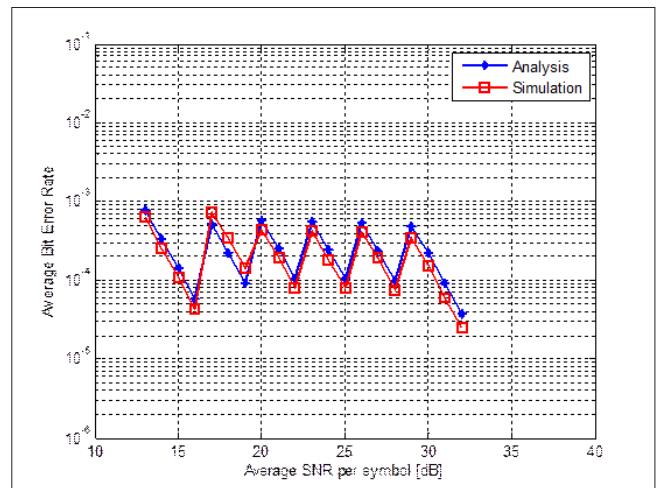
SNR, signal-to-noise ratio.

FIGURE 9: Average bit error rate of an adaptive M-ary quadrature amplitude modulation scheme over a $m = 2$ Nakagami- m fading channel.



SNR, signal-to-noise ratio.

FIGURE 8: Average bit error rate of an adaptive M-ary quadrature amplitude modulation scheme over a $m = 1$ Nakagami- m fading channel.



SNR, signal-to-noise ratio.

FIGURE 10: Average bit error rate of an adaptive M-ary quadrature modulation scheme over a $m = 5$ Nakagami- m fading channel.

for M-QAM, $M = 4, 8, 16, 32, 64$ and 128 over $m = 1, 2$ and 5 Nakagami- m fading channels are plotted in Figures 5, 6 and 7, respectively. The QoS BER target (BER_0) is set to 1×10^{-3} . Because it is not possible to get a simple BER expression which is similar to [Eqn 4], numerical analysis is used to determine the boundary points. The bin thresholds are shown in Table 1.

Finally, simulation results are presented to demonstrate the improved accuracy of the adaptive M-QAM modulation scheme over a Nakagami- m fading channel. The BER performance of the system shows that the proposed scheme meets its BER target of 1×10^{-3} . Figures 8, 9 and 10 show that there is a much tighter fit between the analytical expression and simulation curves for Nakagami- m , $m = 1$ than those of previous studies referenced. Figures 8, 9 and 10 also demonstrate that the system BER_0 target is met throughout the operable SNR range for $m = 1, 2$ and 5 . Unlike the results presented by Goldsmith and Chua³, Figure 8 shows that there is no transmission below the SNR point γ_2 , which

corresponds to the instantaneous SNR boundary for 4-QAM. For a Nakagami- m fading channel, transmitting below this SNR point using 4-QAM will result in an average BER value higher than the BER_0 target. The graph also shows that the average BER performance higher than γ_7 is dominated by the highest modulation mode (128-QAM) of the adaptive scheme.

Conclusion

We investigated the accuracy of a commonly used approximate BER expression for M-QAM in a fading channel. The inaccuracy of the approximate expression was demonstrated via accurate simulations over a slowly varying Nakagami- m block-fading channel. It was also shown that the threshold points for an adaptive M-QAM system derived using the approximate BER expression lead to inappropriate operation of the system in a fading channel. To improve the accuracy of the system BER performance the average BER over a Nakagami- m fading channel was re-derived using



TABLE 1: Boundary points for an adaptive M-ary quadrature amplitude modulation scheme over $m = 1, 2$ and 5 Nakagami- m fading channels.

Mode (n)	Mn	Signal-to-noise ratio (dB)		
		$m = 1$	$m = 2$	$m = 5$
2	4-QAM	26.96	17.40	12.64
3	8-QAM	30.67	21.50	16.93
4	16-QAM	32.49	23.67	19.25
5	32-QAM	35.02	26.50	22.23
6	64-QAM	37.52	29.29	25.14
7	128-QAM	40.05	32.06	28.03

two alternative approximate BER expressions for M-QAM in AWGN. The threshold values for the adaptive M-QAM system were then determined using one of the average BER expressions. Finally, simulation results were used to verify the accuracy of the new threshold points and the new average BER expression over the Nakagami- m fading channel.

Acknowledgements

We thank Professor Guiseppe Abreu who made the code to simulate his proposed system available on his website along with his papers.

References

- Alouini MS, Goldsmith AJ. Adaptive modulation over Nakagami fading channels. *Kluwer J Wireless Commun.* 2000;13(1-2):119-143.
- Chen X, Chat CC, Chew YH. Performance of adaptive MQAM in cellular system Nakagami fading and log-normal shadowing. Paper presented at: PIMRC 2003. Proceedings of the 14th IEEE Personal, Indoor and Mobile Radio Communications Conference; 2003 Sept 7-10; Beijing, China. Piscataway: IEEE Press; 2003. p. 1274-1278.
- Goldsmith AJ, Chua SG. Variable-rate variable-power MQAM for fading channels. *IEEE Trans Commun.* 1997;45(10):1218-1230.
- Goldsmith AJ, Chua SG. Adaptive coded modulation for fading channels. *IEEE Trans Commun.* 1997;46(5):595-602.
- Hole KJ, Holm H, Oien GE. Adaptive multidimensional coded modulation over flat fading channels. *IEEE J Sel Areas Commun.* 2000;18(7):1153-1158.
- Holm H, Hole KJ, Oien GE. Spectral efficiency of variable-rate coded QAM for flat fading channels. Paper presented at: NORSIG 1999. Proceedings of the Nordic Signal Processing Symposium; 1999 Sept 9-11; Asker, Norway. Trondheim: IEEE Press; 1999. p. 130-135.
- Hole KJ, Oien GE. Adaptive coding and modulation: A key to bandwidth-efficient multimedia communications in future wireless systems. *Teletronikk.* 2001;97(1):49-57.
- Liu Q, Zhou S, Giannakis GB. A cross-layer scheduling with prescribed QoS guarantees in adaptive wireless networks. *IEEE J Sel Areas Commun.* 2005;23(5):1056-1065.
- Liu Q, Wang X, Giannakis GB. A cross-layer scheduling algorithm with QoS support in wireless networks. *IEEE Trans Veh Tech.* 2006;55(3):839-847.

- Quazi T, Xu H, Takawira F. Quality of service for multimedia traffic using cross-layer design. *IET Commun J.* 2009;3(1):83-90.
- Yang HC, Belhaj N, Alouini MS. Performance analysis of joint adaptive modulation and diversity combining over fading channels. *IEEE Trans Commun.* 2007;55(3):520-528.
- Kim Y, Hwang GU. Performance analysis of M-QAM scheme combined with multiuser diversity over Nakagami- m fading channels. *IEEE Trans Veh Tech.* 2008;57(5):3251-3257.
- Holter B, Oien GE. Performance analysis of a rate-adaptive dual-branch switched diversity system. *IEEE Trans Commun.* 2008;56(12):1998-2001.
- Gjendemsjo A, Yang H, Oien GE, Alouini MS. Joint adaptive modulation and diversity combining with downlink power control. *IEEE Trans Veh Tech.* 2008;57(4):2145-2152.
- Nechiporenko T, Phan KT, Tellambura C, Nguyen HH. Performance analysis of adaptive M-QAM for Rayleigh fading cooperative systems. Paper presented at: IEEE ICC 2008. Proceedings of the IEEE International Conference on Communications; 2008 May 19-23; Beijing, China. Piscataway: IEEE Press; 2008. p. 3393-3399.
- Abreu G. Accurate simulation of piecewise continuous arbitrary Nakagami- m phasor processes. Paper presented at: IEEE Globecom 2006. Proceedings of the IEEE Global Conference on Telecommunications - Communication Theory Symposium; 2006 Nov 27-Dec 1; San Francisco, USA. Piscataway: IEEE Press; 2006. p. 1-6.
- Proakis JG. Digital communications. New York: McGraw-Hill Inc.; 2001.
- Simon MK, Alouini MS. Digital communications over fading channels. New York: Wiley & Sons Inc.; 2000.
- Chiani M, Dardari D, Simon MK. New exponential bounds and approximations for the computation of error probability in fading channels. *IEEE Trans Commun.* 2003;2(4):840-845.
- Al-Shahrani I. Performance of M-QAM over generalized mobile fading channels using MRC diversity. MSc thesis, Riyadh, King Saud University, 2007.

Appendix I

Derivation of the integral for [Eqn 5]:

$$\begin{aligned}
 & \int_0^{\infty} \gamma^{m-1} \exp(-\gamma\beta) d\gamma \\
 &= \left(\frac{1}{\beta}\right)^{m-1} \int_0^{\infty} \gamma^{m-1} \exp(-\gamma\beta) (\beta)^{m-1} d\gamma \\
 &= \left(\frac{1}{\beta}\right)^{m-1} \int_0^{\infty} (\gamma\beta)^{m-1} \exp(-\gamma\beta) d\gamma \\
 & \text{let } \alpha = \gamma\beta, d\gamma = 1d\alpha \\
 &= \left(\frac{1}{\beta}\right)^{m-1} \int_0^{\infty} (\alpha)^{m-1} \exp(-\alpha) (1) d\alpha \\
 &= \left(\frac{1}{\beta}\right)^{m-1} \int_0^{\infty} (\alpha)^{m-1} \exp(-\alpha) d\alpha \\
 &= \left(\frac{1}{\beta}\right)^{m-1} \Gamma(m)
 \end{aligned}$$